Lab on a Chip

Cite this: *Lab Chip*, 2012, **12**, 1119

www.rsc.org/loc

PAPER

Progress toward multiplexed sample-to-result detection in low resource settings using microfluidic immunoassay cards†

Lisa Lafleur,*[a] Dean Stevens,[b] Katherine McKenzie,[b] Sujatha Ramachandran,[b] Paolo Spicar-Mihalic,[c] Mitra Singhal,[d] Amit Arjyal,[e] Jennifer Osborn,[b] Peter Kauffman,[b] Paul Yager[b] and Barry Lutz[b]

Received 12th August 2011, Accepted 10th January 2012
DOI: 10.1039/c2lc20751f

In many low resource settings multiple diseases are endemic. There is a need for appropriate multi-analyte diagnostics capable of differentiating between diseases that cause similar clinical symptoms. The work presented here was part of a larger effort to develop a microfluidic point-of-care system, the DxBox, for sample-to-result differential diagnosis of infections that present with high rapid-onset fever. Here we describe a platform that detects disease-specific antigens and IgM antibodies. The disposable microfluidic cards are based on a flow-through membrane immunoassay carried out on porous nitrocellulose, which provides rapid diffusion for short assay times and a high surface area for visual detection of colored assay spots. Fluid motion and on-card valves were driven by a pneumatic system and we present designs for using pneumatic control to carry out assay functions. Pneumatic actuation, while having the potential advantage of inexpensive and robust hardware, introduced bubbles that interfered with fluidic control and affected assay results. The cards performed all sample preparation steps including plasma filtration from whole blood, sample and reagent aliquoting for the two parallel assays, sample dilution, and IgG removal for the IgM assays. We demonstrated the system for detection of the malarial pfHRPII antigen (spiked) and IgM antibodies to *Salmonella* Typhi LPS (patient plasma samples). All reagents were stored on card in dry form; only the sample and buffer were required to run the tests. Here we detail the development of this platform and discuss its strengths and weaknesses.

Introduction

Infectious diseases are responsible for approximately 1/3 of deaths in developing countries.[1] In many cases, these diseases are treatable or manageable using available medications, but a primary obstacle to treatment in low-resource settings (LRSs) is correct and timely diagnosis.[2–5] Further, LRSs are often plagued by multiple diseases that share common symptoms, and diagnosing the true cause of infection is difficult based on clinical assessment alone. For example, in malaria-endemic regions, patients presenting with fever are often treated with anti-malarial drugs by default, despite the significant likelihood that the illness is caused by a different pathogen[6–8] or the patient has more than one infection.[9–11] As a result, the medications are used inefficiently, patients do not receive needed treatment, and improper use of therapeutic drugs accelerates the emergence of resistant pathogens. It is widely recognized that there is a need for diagnostics that meet the ASSURED criteria: affordable, sensitive, specific, user-friendly, rapid, equipment-free, and delivered to those who need it.[12,13]

A large number of microfluidic immunoassays have been developed, many targeted at low-resource settings.[3,4,14] Hundreds of blood-based microfluidic immunoassays have been developed,[15] however only a few have been complete sample-to-result systems capable of testing sera samples[16,17] or whole blood samples.[18–21] Multi-analyte detection from whole blood in a point-of-care (POC) device has been achieved for antibody detection,[22] however there is an additional need for multi-analyte diagnostics that are capable of detecting multiple classes of analytes and differentiating between infections that cause similar clinical symptoms. As described below, multi-analyte detection presents special challenges because the preferred diagnostic targets for each pathogen often require different sample preparation steps and assay formats that may be difficult to implement in a single device.

[a]*Department of Electrical Engineering, University of Washington, Seattle, WA, USA. E-mail: llafleur@u.washington.edu; Fax: +01 (206)543-3842; Tel: +01 (206)616-1928*
[b]*Department of Bioengineering, University of Washington, Seattle, WA, USA*
[c]*Department of Chemistry, University of Washington, Seattle, WA, USA*
[d]*PATH, Seattle, WA, USA*
[e]*Oxford University Clinical Research Unit-Patan Academy of Health Sciences, Kathmandu, Nepal*

† Electronic supplementary information (ESI) available. See DOI: 10.1039/c2lc20751f

The work presented here was part of a collaborative project to design a microfluidic POC platform, the DxBox, for sample-to-result differential diagnosis in LRSs.‡ The platform model is a disposable card containing on-board reagents and a portable instrument that automates operation for ease-of-use. The project goal was to develop rapid nucleic acid amplification tests and rapid immunoassays for the identification of multiple pathogens that cause rapid-onset high fever as the primary symptom. The work presented here is one of three approaches for performing immunoassays that were developed during the DxBox project. One system was based on surface-plasmon resonance imaging using a low-cost light source,[23] and the other was a microfluidic enzyme-linked immunosorbent assay (ELISA) format carried out on a patterned plastic substrate [unpublished results from Micronics]. The approach presented here uses a flow-through membrane immunoassay format for high-surface area capture and rapid binding.

Many infectious diseases can be identified in their early stage by immunoassays that detect either pathogen-specific antigens or host-generated IgM antibodies (in contrast, IgG antibodies are typically indicators of past infection or vaccination). To develop microfluidic immunoassay cards for the differential diagnosis of fever, the project team chose a target panel that included antigens generated by malaria parasites (*Plasmodium falciparum* HRPII and pan-malarial aldolase) and host-generated IgM antibodies specific to typhoid, Rickettsia, dengue, and measles infections. We first developed bench-top protocols individually for each target using a common set of conditions (including materials, surface passivation procedures, buffer composition, and assay time) to allow multiplexing of several targets in a single microfluidic card. However, integrating antigen and IgM assays presents an additional challenge because they require different sample preparation steps. For antigen detection, plasma from filtered blood is normally tested without further treatment, while IgM detection normally requires additional steps of sample dilution and the removal of IgG antibodies prior to the assay.[24,25] We designed a microfluidic card to carry out all steps for sample preparation and parallel detection of multiple antigen and IgM targets from a blood sample.

The cards are based on a rapid flow-through membrane immunoassay (FMIA) that integrates desirable features of the classic laboratory ELISA and lateral flow tests (LFTs). Like ELISA, the FMIA allows for multiple independent assay steps separated by washes to reduce non-specific signal.[26] Like LFTs, the FMIA provides a high capture surface area that allows visual detection using coloured labels, and the FMIA allows shorter assay times due to fast diffusion across small membrane pores and delivery of fresh sample to the capture surface by flow. ELISA typically takes 3+ hours due largely to slow diffusion between the bulk fluid and the capture surface, while all the processing and assay steps in the FMIA were complete in about 30 min.

Early in the project, pneumatic fluid actuation was chosen as the basis for this platform. Compared to syringe pumps used in typical microfluidic systems, pneumatic control has the potential to be lower in cost; there is no contact of fluids with the hardware, which could improve instrument reliability. In addition, two-phase flow can be useful for shuttling small fluid volumes without dilution or dispersion that would occur in liquid-driven systems. However, pneumatic operation required development of fluidic control methods, and the inherent conditions for bubble formation were a challenge for robust operation. We describe the pneumatic control methods developed for this project, the potential advantages of pneumatics, as well as the remaining challenges to improve robustness of fluidic control.

The FMIA cards performed twenty separate fluidic operations to carry out all sample processing and assay steps for: 1) detection of pathogen-specific antigens in undiluted samples and 2) detection of human-generated IgM antibodies in diluted samples with pre-assay depletion of IgG antibodies (assay interferent). Each parallel assay mimicked the multi-step protocols used for laboratory immunoassays by delivering sample, washes, and detection reagents in a timed sequence. All chemical reagents were stored dry inside the cards; only the addition of sample and buffer was required to run the assays. Some pieces of this work are established technology (*e.g.* using air vents to meter fluids in channels/chambers). We have previously published some components of this work (*e.g.* the FMIA assay format in bench-top[27] and syringe-driven formats,[28] reagent drying,[28] and IgG removal in an air-driven mixer[29]). This manuscript describes additional fluidic control components, the integration of all components into a single sample-to-result test card, and the results of testing antigen and antibody samples.We demonstrate the card's capabilities by detecting the malarial antigen pfHRPII and IgM antibodies to *Salmonella* Typhi (*S.* Typhi-IgM) from spiked and clinical human samples. Rapid detection of antigen targets and IgM antibody targets in a single platform could improve the ability of healthcare providers to properly treat patients in LRSs where multiple infectious diseases are common.

Experimental

Card fabrication

The assay cards were fabricated by a rapid prototyping method using Mylar laminate layers (Melinex 515, Fralock, Canoga Park, CA), some of which were pre-coated with pressure-sensitive adhesive (T5501, 1 mil, Fralock), and cast acrylic (8505K817, McMaster Carr, Atlanta, GA). The materials were cut using a CO_2 laser (M360, Universal Laser System, Inc., Scottsdale, AZ). Each layer was blocked in 10% bovine serum albumin for 30 minutes on a shaker, rinsed in DI water, and air dried before assembly. Layers were pressed together at 1600 psi (International Crystal Labs, Garfield, NJ) to form microchannels. Four types of membranes were used in the cards: nitrocellulose assay membranes (Protran 0.45 μm pore size, Whatman, Maidstone, Kent, UK), blood filtration membranes (Vivid™, Pall Corp., Port Washington, NY), polyester mesh as a bead filter (Pall Corp), and air permeable membranes (Mupor PM3V, Interstate Specialty Products, Sutton, MA). The pressures used on-card sometimes exceeded the Laplace pressure of the pores in the air-permeable membranes, which resulted in fluid break-through. It is advisable to use membranes with smaller pores to prevent fluid break-through. Most membranes were

‡ The DxBox Project, as it was informally called, was funded by a grant from the Bill & Melinda Gates Foundation through their Grand Challenges in Global Health initiative.

laser-cut, but the air-permeable membranes were cut by hand (laser-cutting of Teflon may generate toxic gases). Membranes were integrated by sandwiching each membrane between laminate layers during assembly. The blood filtration membrane had a surface area of 1.15 cm^2 and a capacity to filter 40–50 μL blood/cm^2. The cards were a total of 23 layers including on-card pneumatically-actuated valves (Micronics, Inc., Redmond, WA).

Assay substrate preparation

Capture reagents were patterned on nitrocellulose assay membranes with a robotic piezoelectric spotter (Scienion sciFLEXARRAYER S3, Dortmund, Germany). To capture the target antigen, anti-pfHRPII IgM (MPFM-55A, Immunology Consulting Labs, Inc., Newberg, OR) was spotted at 0.5 mg mL^{-1} in phosphate buffered saline (PBS). For the antigen process control, bovine serum albumin conjugated to biotin (AGBIO-0100, Arista, Allentown, PA) was spotted at 0.25 mg mL^{-1} in PBS. To capture the IgM target, the antigen lipopolysaccharide from *S.* Typhi (L7895, Sigma, St. Louis, MO) was spotted at 1 mg mL^{-1} in PBS. For the IgM process control, human IgM (I8260, Sigma) was spotted at 0.25 mg mL^{-1} in PBS, and for the endogenous control anti-human IgM $Fc_{5\mu}$ (109-006-129, Jackson Immunoresearch, West Grove, PA) was spotted at 0.25 mg mL^{-1} in PBS. Membranes were spotted with all capture reagents (30 nL/spot; 80 drops, ~375 pL/drop), dried for 30 min, soaked in a membrane surface passivation solution (00-0105, Invitrogen, Carlsbad, CA) for 60 min, and stored dry in a desiccator until use.

Samples for card testing

The target analyte for the typhoid assay was IgM antibody generated by the human host; there are no sources of purified disease-specific human IgM (as would be used to create spiked samples of known analyte concentration), so assays were tested using a panel of patient samples that were characterized by laboratory ELISA.

Specimens for platform testing were collected as part of a randomized controlled trial (Current Controlled Trials ISRCTN 53258327; human subjects approvals: OXTREC 002-6 and HS 393) from patients presenting to Patan Hospital in Kathmandu, Nepal with typhoid fever. Plasma was separated from blood cells by centrifugation and stored at −20 °C until use. Whole blood used as a sample matrix for spiked composite samples was collected from uninfected individuals at the University of Washington Medical Center Blood Draw Lab (human subjects approval: UW 35076).

For the *S.* Typhi IgM assay, we tested a blinded panel of nine clinical plasma samples that included specimens identified as positive or negative by laboratory ELISA performed by PATH (Seattle, WA). Signal indicated the presence of anti-LPS *S.* Typhi IgM (*S.* Typhi-IgM). For the malaria antigen assay, recombinant pfHRPII antigen (20050, ImmunoDiagnostics, Woburn, MA) was spiked into fetal bovine serum (FBS) (Invitrogen).

For the antigen assay and control, two detection reagents were used: anti-pfHRPII IgG (MPFG-55A, Immunology Consulting Labs) conjugated to gold (Au) nanoparticles (custom conjugation, BBInternational, Cardiff, United Kingdom) to bind to the target pfHRPII antigen and Au-streptavidin (CGSTV-0600, Arista Biologicals) to bind to the process control spot. The IgM assays and controls used a single detection reagent: anti-human IgM $Fc_{5\mu}$ was conjugated to gold nanoparticles (custom conjugation, Arista Biologicals). The gold-antibody detection reagents (Au–Ab) were dried on laser-cut polyester conjugate pads in the presence of trehalose at 10% w/v,[28] stored dry on-card, and reconstituted with buffer during the assay. Buffer for washes (200 μL per circuit) and reconstitution (100 μL per circuit) was Tris-buffered saline + 0.1% Tween-20 (TBST).

Clinical samples infected with both malaria and *S.* Typhi were not available, so composite samples were prepared. Whole blood was collected in tubes containing EDTA then centrifuged at 5000 rpm to separate the plasma from blood cells which were recombined into composite samples containing controlled fractions of *S.* Typhi-infected plasma, blood cells, and spiked antigen.

IgG removal

The sample for IgM testing was pre-conditioned on-card by removing IgG antibodies (assay interferent) through a selective binding reaction with protein G-coated beads (UltraLink® resin, Pierce, Rockford, IL). 50 μL of beads in DI water with 80% sucrose were deposited in the mixing chamber and dried prior to card assembly.[29]

Pneumatic actuation control system

A custom pneumatic actuation control system (PACS) was fabricated based on the DxBox alpha prototype system designed by Micronics. The PACS hardware included two air pumps (vacuum and pressure), plastic bottles (accumulators to reduce pressure fluctuations), solenoid-actuated air valves (thirteen), and an electronic controller to actuate the valves. The PACS controlled eight air lines for on-card valving and five air lines for driving fluids. The PACS was comprised of two in-house fabricated logic boards (WTDIO-M, Weeder Technologies, Fort Walton Beach, FL) controlled through a terminal emulator (Indigo, shadeBlue LLC, TX) which allowed time delays to be intermixed with the serial board commands required to change the valve and driving line states. The PACS airlines were switched with pneumatic 2-way toggle valves (LHDA1231115H 12 VDC, Lee, Essex, CT). The air sources (AP120DEEEF60C3, Sensidyne, Clearwater, FL) were down-regulated (Airtrol, New Berlin, WI) to the desired pressures of ±10 psi for on-card valves, and pressures of ±1 psi or atmosphere for the fluid driving lines.

Image analysis

Membranes were imaged by a web cam (Pro 9000, Logitech, Fremont, CA) during the assay, then were disassembled after the assay to be imaged on a flatbed scanner (ScanMaker i900, MicroTek International, Inc., Cerritos, CA) in 48-bit-depth RGB at a resolution of 1200 dpi. Spot signals and background signals were quantified as the green channel intensity,[30] which is the region of the visual spectrum with the largest dynamic range for imaging the red-colored Au labels. The raw intensities of the image (16-bits per channel) were normalized to give a scale representing pure white as 0 and pure black as 1 ([(65535-intensity)/65535]). The assay signal presented for each spot was the

normalized intensity of that spot minus the normalized intensity of the local background. Webcam images were not used for image quantification because a portion of the card blocked uniform lighting (a fixable feature); scanner images were used for image quantification. We compared quantification for the scanner and webcam by imaging an intensity standard and calculating intensities using the same method as for assay quantification; with uniform lighting (as would occur in the DxBox instrument) the webcam gave signal intensities within 4% of the scanner across the full spectrum of grayscale intensities.

Results and discussion

On-card immunoassay process

Fig. 1 summarizes the assay operations performed on card. First, a blood sample was loaded and drawn through a size-exclusion plasma extraction membrane to remove cells. The total plasma filtration time was approximately five minutes (at 1 psi vacuum). The plasma sample was divided into two channel segments with fixed volumes: one aliquot for the antigen assay (50 μL) and one aliquot (2 μL) to be further processed for the IgM assay.

The IgM indirect assay format used here has the advantage of allowing multiplexing (see below), but it also required a dilution step and removal of IgG antibodies that generate false positive and false negative reactions.[25] On the card, the 2 μL sample aliquot for IgM analysis was first diluted in buffer (1 : 100), mixed with IgG binding beads (5 min), and filtered to produce an IgG-depleted sample ready for the IgM indirect assay. These steps were carried out using a novel air-driven batch mixer described below.

After initial processing, the multi-step assays for antigen and IgM detection were carried out in parallel through fluidically-isolated regions of the capture membrane. A three-component stack was created to detect each target analyte, and each reagent delivery step was followed by a wash step to remove unbound sample/labels. For the antigen assay, pre-spotted anti-pfHRPII antibody captured the pfHRPII antigen from the sample. Captured antigen was labelled with gold conjugated to a different anti-pfHRPII antibody. For the IgM assay, pre-spotted *S.* Typhi LPS antigen captured *S.* Typhi-IgM from the sample. Captured IgM was labelled by gold conjugated to a pan-IgM detection antibody. This "indirect" IgM assay format was chosen because it allows multiplexing of IgM targets with a single detection label. Specificity for each IgM target in a multiplexed assay is achieved by spotting pathogen-specific capture antigens at different locations on the assay membrane.

All chemical reagents were stored on card in dry form. The capture reagents for assay targets and controls were pre-spotted on the assay membrane and dried before card fabrication. The detection reagents and IgG removal beads were dried in sugar for chemical preservation and rapid dissolution by buffer during the assay. The IgG removal beads dried in sugar were shown to be stable for >1 month at 45 °C.[29] Au–Ab conjugates dried in conditions similar to those used in this paper were shown to retain 80–96% of their activity after 60 days at elevated temperature.[28]

Card design and operation using pneumatics

These microfluidic cards were controlled by a pneumatic system that used air pressure and vacuum to drive fluid movement and operate on-card valves in conjunction with air-permeable vents, which pass air but not aqueous fluids. Pneumatics can be well suited for handling small fluid volumes and interfacing with fully-integrated cards. In addition, pneumatics can be well suited to shuttling small fluid volumes (in two directions) without dilution or Taylor dispersion. A potential disadvantage is that

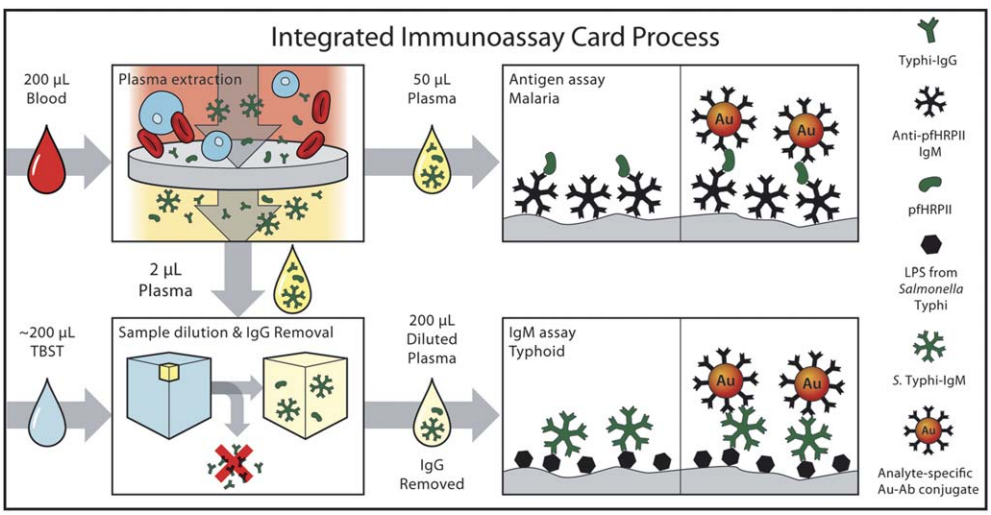

Fig. 1 Process flow of the DxBox integrated immunoassay cards. A blood sample was added to the card and drawn through a plasma extraction membrane to remove blood cells. The plasma was aliquoted into two sample volumes: 50 μL for antigen detection and 2 μL for IgM detection. The IgM sample required further processing: it was diluted with buffer (1 : 100 in TBST) and mixed with protein-G beads (5 minutes) to selectively remove IgG antibodies (assay interferent). Then, the antigen sample and processed IgM sample were pushed transversely through the assay membrane where immobilized reagents captured the target analytes (malaria antigen and *S.* Typhi-IgM). Each target was labeled with gold (Au) nanoparticles conjugated to detection antibodies. All processes from sample to result were carried out on card. All reagents were contained on the cards in dry form; only sample and buffer needed to be supplied to run the assays.

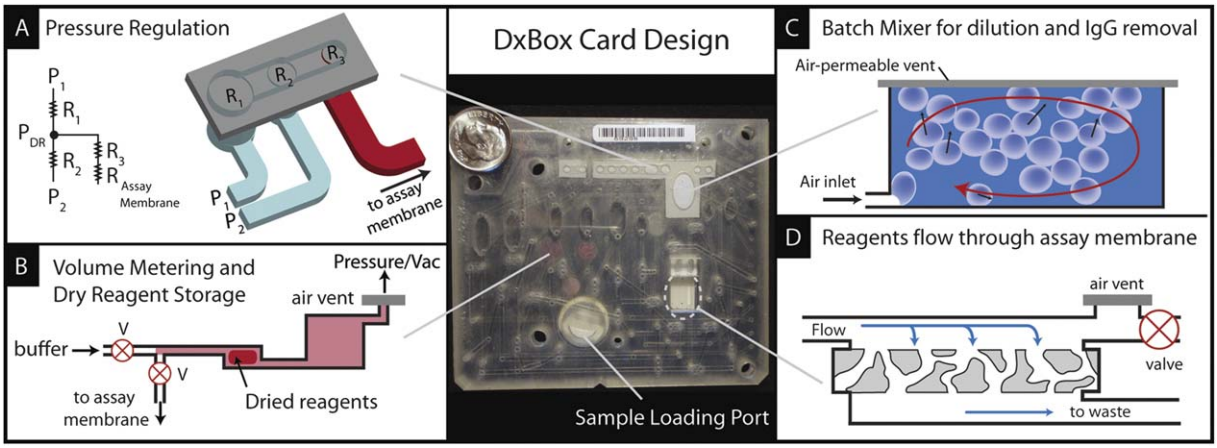

Fig. 2 Photograph of the integrated microfluidic card and illustrations of processes designed for fluid manipulation by pneumatic control. The pneumatically-controlled cards used hydrophobic membranes as air-permeable vents to carry out some key functions illustrated here. A) Schematic of on card pressure regulation used to generate additional driving pressures to set flowrates for optimal contact time (sample and detection reagents) or assay speed (washes). B) Air sources do not control fluid volume directly, so each reagent volume was aliquoted in a pre-defined channel on-card for reproducible assays. C) A batch mixer actuated by air was used for sample dilution and IgG removal (vital sample processing steps in the IgM assay). Air was used to drive fluids creates bubbles that rise through the chamber and exit through an air-permeable vent at the top. The bubble motion created mixing throughout the chamber. D) Schematic of the assay membrane region and the air vent used to remove the air between reagent deliveries. The valve was used to clear fluid from the vent between steps.

pneumatics does not provide direct control over flowrates or fluid volumes, as can be easily done with syringe pumps. Also, the air-liquid interface can create bubbles that interfere with fluidic control. Driving fluids with air sources required methods to aliquot consistent fluid volumes, tune air pressures to optimize fluid flowrates, mix reagents, and vent air bubbles created by the air source. Fig. 2 shows a photograph of a DxBox card and depicts several structures designed for fluidic control in pneumatically-driven systems.

An on-card pressure regulator was developed to allow a single air pump to provide additional driving pressures on demand. The regulator principle is analogous to a voltage divider in an electric circuit (Fig. 2A). The desired driving pressure on-card, P_{dr}, was a function of the source pressures and the ratio of the areas of two air-permeable vents, $P_1 - P_{dr} = (P_1 - P_2)*(R_1/(R_1 + R_2))$, where R_1 and R_2 are proportional to the vent areas (4.8 and 7.5 mm^2, respectively). On the PACS, the pressure regulator allowed selection between 1 psi pressure, 1 psi vacuum and atmosphere. The possible outputs from multiplexing these input combinations were 1 psi, ~0.6 psi, ~0.4 psi, and atmosphere. The pressure modulation was used to reduce assay time by washing at a higher pressure, while the sample and detection reagents were driven at a lower pressure to provide the desired contact time with the assay membrane.

Sample, wash, and reagent volumes were aliquoted by drawing buffer into vented chambers of defined volume, and then each fluid was sequentially delivered by applying pressure to the vent (Fig. 2B). Buffer was aliquoted into channels containing the dry reagents to generate an assay-ready liquid reagent.

The IgM assays required a batch mixer to carry out the sample dilution and bead-based IgG removal steps. Batch mixing of reagents is ubiquitous in laboratory assays; however, we found no examples of microfluidic batch mixers that could be driven by an air source. Thus, we developed a batch mixer that uses bubbles to drive mixing in a chamber with a vented ceiling (Fig. 2C). We previously characterized the efficiency of the mixer and measured the effectiveness of bead-based IgG removal.[29]

Pneumatic fluid control inherently led to air gaps between fluids after each step and introduced bubbles that could interfere with fluid flow through the assay membrane. The assay membrane bubble point was greater than the pressures used on

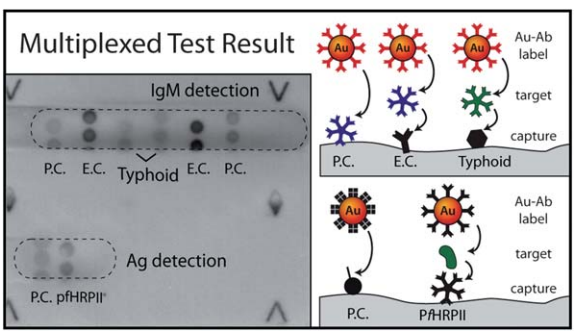

Fig. 3 Detection of antigens (malarial pfHRPII) and IgM antibodies (*S.* Typhi-IgM) from a single blood sample in a DxBox card. Two fluidically-isolated detection windows were used for IgM detection (top) and antigen detection (bottom), with control assays in each window. The result shown is for a composite sample made up of a typhoid-positive clinical plasma sample (179 μL), a cell slurry from fresh blood (20 μL), and spiked pfHRPII antigen (500 ng mL^{-1}).The labels on the membrane image indicate the location of each pre-spotted capture reagent for the targets, the process controls (P.C.), and the endogenous control (E.C.). For the IgM assays, the *S.* Typhi-IgM is shown in green and generic human IgM (not specific to *S.* Typhi) is shown in blue. A single detection reagent (Au-anti-human-IgM) was used for all labeling. For the antigen assay, a pre-spotted capture antibody (anti-pfHRPII) captured the pfHRPII target, which was labeled by an analyte-specific label (Au-anti-pfHRPII). For the antigen process control, pre-spotted biotinylated BSA bound Au-streptavidin. The two detection labels for the antigen assay were stored in dry form on separate pads on the card but were rehydrated and applied as a single fluid reagent.

card, so bubbles or air plugs could not be passed through the membrane. A hydrophobic vent near the assay membrane (Fig. 2D) allowed the removal of air between each fluid delivery step. Similar vent membranes have been used in other microfluidic cards to remove air bubbles.[31]

Non-uniformities in the surface energy of the channels can lead to fluid spontaneously stopping in channels when the driving pressure is below a certain threshold. The desired sample and reagent contact times required using driving pressures at or near that minimum pressure threshold when unblocked cards were used. Channel surface passivation has the benefit of reducing non-specific binding of sample and reagents, but it also improved the surface uniformity and allowed fluids to be driven at low pressures.

Multi-analyte detection from blood

Fig. 3 shows an assay membrane image from a card used for detection of pfHRPII antigen and *S.* Typhi-IgM from a composite blood sample and a graphical representation of each reagent stack in the assays. The cards contained all reagents in dry form, and were run by adding the sample and a buffer solution. All steps including sample filtration, aliquoting, dilution, IgG removal, reagent rehydration, and the multi-step assay were carried out on the cards. The IgM assay window (upper) included spots for the IgM process control (confirmed exposure to detection labels), the IgM endogenous control (confirmed exposure to a human blood/plasma sample), and the IgM target analyte (*S.* Typhi-IgM). The antigen assay window (lower) included spots for the process control (confirmed exposure to detection labels) and the antigen target analyte (pfHRPII). The smaller antigen detection window was used to increase the amount of target flowing through the capture spots for improved sensitivity. Control spots allowed the test to be rejected in the event of card failure or if the user loaded a sample other than human blood or plasma onto the card. To evaluate the card performance, cards were tested separately for *S.* Typhi-IgM detection and pfHRPII detection, as described below.

IgM antibody detection: typhoid fever

The cards were evaluated by testing a set of samples on the cards (one card per sample) and comparing to results for the same samples run in a bench-top version of the FMIA and by laboratory ELISA. The test panel was chosen from set of samples that included both negative samples and positive samples with a range of responses in ELISA. It is important to note that the

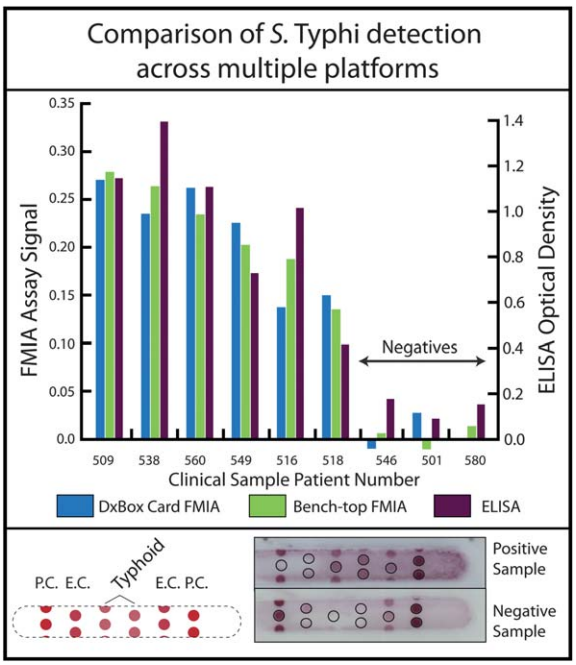

Fig. 4 Comparison of *S.* Typhi-IgM detection across multiple platforms. The IgM assay window included spots for a process control (P.C.), an endogenous control (E.C.), and the typhoid target (*S.* Typhi-IgM). The membranes images are examples of positive and negative *S.* Typhi-IgM samples (as determined by laboratory ELISA). The graph shows the results for a panel of positive and negative clinical samples tested on card (blue bars), in the bench-top FMIA (green bars), and by laboratory ELISA (purple bars). The data points for the bench-top and on-card FMIA represent single measurements from patient samples; the volume of each sample was limited and was not sufficient to perform replication measurements on the cards. The data points for ELISA represent two replicate measurements. The assay cards gave comparable intensity response across the panel of clinical samples.

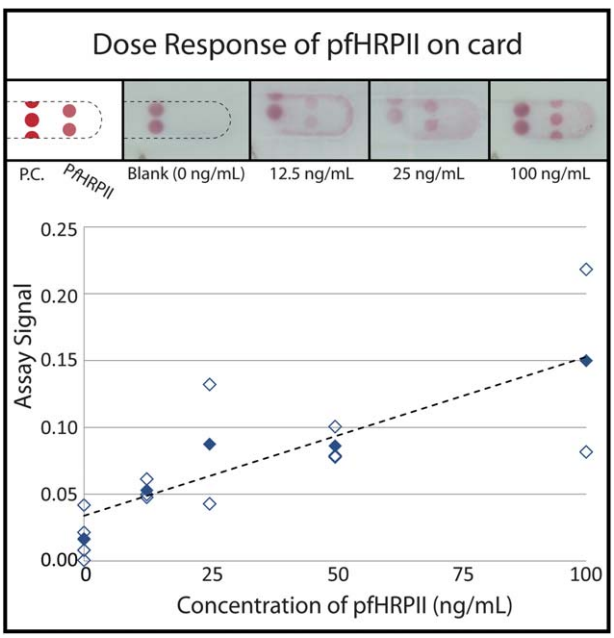

Fig. 5 Antigen detection on the DxBox card. The membrane images show experimental results for pfHRPII antigen spiked into FBS at concentrations between 0 and 100 ng mL^{-1}. The antigen assay window includes a process control (indicates that detection labels were delivered) and the pfHRPII antigen capture spots. A major cause of non-uniformities in the results was the variation in local background sometimes caused by bubbles trapped on the assay membrane. Spot intensities and local background intensities were extracted from membrane images, and the background subtracted assay signal was calculated for each card to generate the plot of assay signal versus spiked antigen concentration. The unfilled points represent individual experiments; the filled points are the average at each concentration. The linear fit is to the average concentrations and had a coefficient of determination, r^2, of 0.9.

small sample set does not allow evaluation of clinical utility; here we perform a limited comparison of assay signals for the three assay formats. Fig. 4 shows the spot pattern for the IgM assay and example membrane images from a strong positive *S.* Typhi-IgM sample and a negative sample.

The following set of criteria was applied to each assay result to define a successful assay. Firstly, the spot intensities were extracted by quantifying signal within an overlaid spotting pattern. If control spots were missing from one side or the other, data from that side was rejected. For example, the positive sample shown here was missing control spots (left side) due to a bubble trapped over part of the assay membrane. Partial, but not complete, bubble obstructions still allowed the target spots to be quantified and the unobstructed control spots to verify a successful test.

In the FMIA we report background-subtracted signal to account for non-specific binding. The positive sample shows significant non-specific signal (reddish color) in non-spotted regions (*i.e.* background). This background is very likely due to non-specific binding of non-target IgM, which is a known source of background in indirect IgM assays. The amount of total IgM is elevated during infection by any pathogen, and it also varies between patients and at different time points during infection. In ELISA, the non-specific binding of IgM can result in false positive results unless separate IgM control wells are tested for each sample. Quantifying background subtracted signal in the FMIA reduced these types of false positives.[27]

Fig. 4 also shows a graph of the quantified assay signal from the on-card FMIA for each clinical sample (blue bars) and compares the results to the bench-top FMIA (green bars) and the optical density from ELISA (purple bars). The DxBox card results showed an intensity response comparable to both the bench-top FMIA and the laboratory ELISA. Plotting the on-card FMIA *versus* ELISA showed a coefficient of determination, r^2, of 0.73 and a standard deviation of errors of 0.07 (24% of maximum on-card FMIA signal). Comparing the on-card FMIA *versus* bench-top FMIA showed a coefficient of determination of 0.92 and a standard deviation of errors of 0.03 (12% of maximum on-card FMIA signal). Calculations and plots are shown in Supplementary Information. These patient samples are part of a larger set. For reference, in ELISA replicate measurements (n = 2 for 15 patients) the average coefficient of variation (CV) found was 8%. Bench-top FMIA replicate measurements (n = 2 for 8 patients) showed an average CV of 15%.[27]

Antigen detection: malaria pfHRPII

The limit of detection (LOD) for laboratory ELISA is near 4 ng mL^{-1},[32] and clinical samples can range from this low level to as high as 10^3 ng mL^{-1}.[33] Fig. 5 shows example membrane images and plots data from individual card runs for samples spiked with recombinant pfHRPII across the low end of the analytical range with two to three replicates tested at each concentration and six blank samples (0 ng mL^{-1}). The assay signal was quantified from the green channel intensity of membrane images; the intensity of unspotted background regions was subtracted from the assay spot intensity to give the reported assay signal. Due to the small sample set, the plot includes both the average signal at each concentration (filled) and individual data points (unfilled). Previously, we showed that syringe pump driven cards gave a pfHRPII dose response curve with low variability[28] and an LOD of 10–20 ng mL^{-1}. In Fig. 5, it is difficult to assign an LOD for these cards due to the small data set and significant variability. Nevertheless, most spiked samples gave signals higher than the set of blanks, and the response curve shows a qualitative correlation with spiked concentration.

In Fig. 5, the variability is due largely to a few card runs that gave aberrant results, and this highlights one of the key problems that affected card robustness. In videos recorded during operation, we sometimes observed bubbles trapped over the assay membrane. Bubbles can be created at any interface of fluids with the driving air, especially at channel intersections and in portions of the card that were filled, emptied, and refilled (*e.g.*, wash channels). Bubbles created upstream of the membrane can affect the flow rates, and thus contact time, of sample and reagents. Bubbles that reach the assay membrane can physically block assay spots (thus reducing signal), or they can block unspotted portions of the membrane leading to increases in contact time (thus potentially increasing signal at assay spots). It is worth noting that the flow-through region of the assay membrane for the IgM assay was 4-fold larger than the antigen assay, so trapped bubbles had a larger impact on the pfHRPII assay. From bench-top experiments, we found that the pfHRPII assay was sensitive to sample contact time in the range of 1–5 min (see Supplementary Information). Sensitivity to contact time could be reduced by running at slower flow rates (at the expense of greater assay time), but ultimately more effective bubble management would be required for robust operation. Despite significant variation between card runs, the data set qualitatively shows detectable responses for samples in the relevant range of analyte concentrations.

Conclusions

The DxBox was designed as a card-plus-reader platform for differential diagnosis of diseases in LRSs. The instrument was designed to be usable in a small clinic setting where sample transport to a centralized laboratory was prohibitive. The inclusion of a battery and no reliance on water make it usable even with minimal laboratory infrastructure. Due to upfront cost and the potential for wear and break down, instrument diagnostics are not optimized for all settings. In the absence of available maintenance, non-instrumented tools would be preferable.

We have developed additional immunoassays from the original fever panel by adapting ELISA protocols into the bench-top FMIA format: an antigen assay for pan-malarial aldolase and IgM assays for diagnosis of typhoid fever,[27] dengue fever, measles, and spotted fever (*Rickettsia*) [unpublished results]. We have previously demonstrated multiplexed antigen detection of pfHRPII and aldolase on an earlier iteration of the assay cards.[34] The FMIA format could be applied to other diagnostic panels, such as diarrheal diseases and sexually transmitted infections, and extended to other sample matrices by adapting existing ELISA protocols. In principle, multiplex detection can be accomplished by simply spotting additional capture molecules for each analyte (and providing additional detection labels for antigen targets). In practice, multiplexing also requires the

challenging task of identifying a single set of assays conditions for all analytes (assay time, surface passivation conditions, buffer composition, *etc.*). For all sample matrices (blood, saliva, urine, *etc.*) the sample viscosity, and variation in viscosity between samples, must be considered in order to achieve target contact times with the assay membrane.

The pneumatic designs presented here for volume metering, flow rate control, and mixing were successful, but the robustness would be improved by better management of bubbles or a design that is more tolerant of bubbles. Similar issues with bubble generation might be faced when using syringe pumps since creating air-free interfaces between fluids would still be required. Potential solutions to this problem would be to include more effective bubble vents[35] (which we explored and rejected due to incomplete bubble removal in this system), or to use an assay membrane that allows air (and air bubbles) to be pushed through without trapping.

The immunoassay card described here was designed to be a true sample-to-result platform capable of carrying out sophisticated multi-step protocols, but this came at a cost. The cards were made from many laminate layers and involved several pick-and-place operations for dry reagent pads and membranes. Complexity in card fabrication can increase risk of card failure; the failure rate due to card leakage was ~4%. The number of laminate layers was due largely to the use of multiple membranes at different planes in the card, the transverse flow geometry of the assay membrane, and the multi-layer sandwich used to hold membranes in place. Other assay cards created for the DxBox system by Micronics did not use membranes and were substantially simpler in structure. For membrane-based cards, injection molded parts with features on both faces could replace multiple laminate layers, and designs that reduce membranes to a single plane within the card could substantially reduce the total number of layers. Nevertheless, the cards as designed surpass typical microfluidic systems by integrating sophisticated sample preparation steps and multi-step assay protocols, resulting in a true sample-to-result system for two parallel multiplexed assays with performance approaching laboratory assays.

Acknowledgements

We gratefully acknowledge the support of The Bill & Melinda Gates Foundation through their Grand Challenges in Global Health Initiative; this project was funded under Grant Number 37884, "A Point-of-Care Diagnostic System for the Developing World," awarded to the UW-led consortium: Paul Yager, PI (UW) and collaborators led by Fred Battrell (Micronics Inc.), Walt Mahoney (Epoch BioSciences), Gonzalo Domingo (PATH), and Patrick Stayton (UW). The views expressed by the authors do not necessarily reflect the views of the funding agency. The authors gratefully thank Micronics for supplying card valve layers made using their proprietary technology; we thank Neil Geisler, Abhishek Choudhary, Devon Cole, and James Wong of UW for fabricating the microfluidic cards. We thank Sugandhan Venkatachalam, and Camille Petri and several of their predecessors in the Yager group for their work on assay development. We thank PATH, Micronics, Epoch Biosciences, and the Stayton Group (UW) for their collaboration and discussions throughout this project. We sincerely thank collaborators at the Oxford University Clinical Research Unit (OUCRU)-Patan Academy of Health Sciences, Kathmandu, Nepal and the Hospital for Tropical Diseases (HTD), Wellcome Trust Major Overseas Programme, Oxford University Clinical Research Unit, Ho Chi Minh City, Vietnam for supplying typhoid clinical samples; specifically we thank Sabina Dongol (OUCRU), Stephen G. Baker (HTD), Buddha Basnyat (HTD), Jeremy Farrar (HTD), and Christiane Dolecek (HTD). We also thank Gonzalo Domingo (PATH) for his review of the manuscript.

References

1 WHO, *The Global Burden of Disease: 2004 Update*, World Health Organization, Geneva, 2008.
2 A. W. Martinez, S. T. Phillips, G. M. Whitesides and E. Carrilho, *Anal. Chem.*, 2010, **82**, 3–10.
3 B. Weigl, G. Domingo, P. LaBarre and J. Gerlach, *Lab Chip*, 2008, **8**, 1999–2014.
4 P. Yager, G. J. Domingo and J. Gerdes, *Annu. Rev. Biomed. Eng.*, 2008, **10**, 107–144.
5 S. R. Jangam, D. H. Yamada, S. M. McFall and D. M. Kelso, *J. Clin. Microbiol.*, 2009, **47**, 2363–2368.
6 R. Joshi, J. M. Colford, A. L. Reingold and S. Kalantri, *Am. J. Trop. Med. Hyg.*, 2008, **78**, 393–399.
7 S. Gwer, C. Newton and J. A. Berkley, *Am. J. Trop. Med. Hyg.*, 2007, **77**, 6–13.
8 H. Reyburn, H. Mbakilwa, R. Mwangi, O. Mwerinde, R. Olomi, C. Drakeley and C. J. M. Whitty, *Br. Med. J.*, 2007, **334**, 403.
9 A. Animut, Y. Mekonnen, D. Shimelis and E. Ephraim, *Jpn. J. Infect. Dis.*, 2009, **62**, 107–110.
10 A. C. Nwuzo, R. A. Onyeagba, I. R. Iroha, O. Nworie and A. E. Oji, *Sci. Res. Essays*, 2009, **4**, 966–971.
11 E. Agwu, J. C. Ihongbe, G. R. A. Okogun and N. J. Inyang, *Braz. J. Microbiol.*, 2009, **40**, 329–332.
12 H. Kettler, K. White and S. Hawkes, *Mapping the landscape of diagnostics for sexually transmitted infections*, WHO, 2004.
13 D. Mabey, R. W. Peeling, A. Ustianowski and M. D. Perkins, *Nat. Rev. Microbiol.*, 2004, **2**, 231–240.
14 C. D. Chin, V. Linder and S. K. Sia, *Lab Chip*, 2007, **7**, 41–57.
15 H. Jiang, X. A. Weng and D. Q. Li, *Microfluid. Nanofluid.*, 2011, **10**, 941–964.
16 W. C. Yang, M. Yu, X. H. Sun and A. T. Woolley, *Lab Chip*, 2010, **10**, 2527–2533.
17 G. A. Messina, N. V. Panini, N. A. Martinez and J. Raba, *Anal. Biochem.*, 2008, **380**, 262–267.
18 J. V. Jokerst, A. Raamanathan, N. Christodoulides, P. N. Floriano, A. A. Pollard, G. W. Simmons, J. Wong, C. Gage, W. B. Furmaga, S. W. Redding and J. T. McDevitt, *Biosens. Bioelectron.*, 2009, **24**, 3622–3629.
19 Z. K. Wang, S. Y. Chin, C. D. Chin, J. Sarik, M. Harper, J. Justman and S. K. Sia, *Anal. Chem.*, 2010, **82**, 36–40.
20 J. Moorthy, G. A. Mensing, D. Kim, S. Mohanty, D. T. Eddington, W. H. Tepp, E. A. Johnson and D. J. Beebe, *Electrophoresis*, 2004, **25**, 1705–1713.
21 B. S. Lee, Y. U. Lee, H. S. Kim, T. H. Kim, J. Park, J. G. Lee, J. Kim, H. Kim, W. G. Lee and Y. K. Cho, *Lab Chip*, 2011, **11**, 70–78.
22 C. D. Chin, T. Laksanasopin, Y. K. Cheung, D. Steinmiller, V. Linder, H. Parsa, J. Wang, H. Moore, R. Rouse, G. Umviligihozo, E. Karita, L. Mwambarangwe, S. L. Braunstein, J. van de Wijgert, R. Sahabo, J. E. Justman, W. El-Sadr and S. K. Sia, *Nat. Med.*, 2011, **17**, 1015–1019.
23 R. Thariani and P. Yager, *PLoS One*, 2010, 5.
24 D. Narayanappa, R. Sripathi, K. JagdishKumar and H. S. Rajani, *Indian Pediatrics*, 2010, **47**, 331–333.
25 T. B. Martins, T. D. Jaskowski, C. L. Mouritsen and H. R. Hill, *Clin. Diagn. Lab. Immunol.*, 1995, **2**, 98–103.
26 D. Stevens, K. Nelson, E. Fu, J. Foley and P. Yager, in *Microfabrication and Microfluidics – Methods in Bioengineering*, ed. J. Zahn, Artech House Inc., Norwood, MA, 2009, pp. 225–244.
27 S. Ramachandran, M. Singhal, K. G. McKenzie, J. L. Osborn, A. Arjyal, S. Dongol, S. G. Baker, B. Basnyat, J. Farrar,

C. Dolecek, G. J. Domingo, P. Yager and B. Lutz, *Journal of Immunological Methods*, 2011.
28 D. Y. Stevens, C. R. Petri, J. L. Osborn, P. Spicar-Mihalic, K. G. McKenzie and P. Yager, *Lab Chip*, 2008, **8**, 2038–2045.
29 K. G. McKenzie, L. K. Lafleur, B. R. Lutz and P. Yager, *Lab Chip*, 2009, **9**, 3543–3548.
30 W. S. Rasband, U. S. ImageJ, *National Institutes of Health*, Bethesda, MD, http://imagej.nih.gov/ij/, 1997–2011.
31 J. Xu, R. Vaillant and D. Attinger, *Microfluid. Nanofluid.*, 2010, **9**, 765–772.
32 C. M. Kifude, H. G. Rajasekariah, D. J. Sullivan, V. A. Stewart, E. Angov, S. K. Martin, C. L. Diggs and J. N. Waitumbi, *Clin. Vaccine Immunol.*, 2008, **15**, 1012–1018.
33 L. Manning, M. Laman, D. Stanisic, A. Rosanas-Urgell, C. Bona, D. Teine, P. Siba, I. Mueller and T. M. E. Davis, *Clin. Infect. Dis.*, 2011, **52**, 440–446.
34 L. K. Lafleur, B. Lutz, D. Stevens, P. Spicar-Mihalic, J. Osborn, K. McKenzie and P. Yager, *MicroTAS*, Jeju, South Korea, 2009.
35 D. D. Meng, J. Kim and C.-J. Kim, *J. Micromech. Microeng.*, 2006, 419.